

# Atoms as electron accelerators for measuring the $e^+e^- \rightarrow \text{hadrons}$ cross section

Fernando Arias-Aragón,<sup>1,\*</sup> Luc Darmé,<sup>2,†</sup> Giovanni Grilli di Cortona,<sup>3,‡</sup> and Enrico Nardi<sup>1,4,§</sup>

<sup>1</sup>*Istituto Nazionale di Fisica Nucleare, Laboratori Nazionali di Frascati, Frascati, 00044, Italy*

<sup>2</sup>*Université Claude Bernard Lyon 1, CNRS/IN2P3,*

*Institut de Physique des 2 Infinis de Lyon, UMR 5822, F-69622, Villeurbanne, France*

<sup>3</sup>*Istituto Nazionale di Fisica Nucleare, Laboratori Nazionali del Gran Sasso, Assergi, 67100, L'Aquila (AQ), Italy*

<sup>4</sup>*Laboratory of High Energy and Computational Physic,*

*HEPC-NICPB, Rõvala 10, 10143, Tallin, Estonia*

(Dated: July 24, 2024)

The hadronic vacuum polarization contribution to  $(g - 2)_\mu$  can be determined via dispersive methods from  $e^+e^- \rightarrow \text{hadrons}$  data. We propose a novel approach to measure the hadronic cross section  $\sigma_{\text{had}}(s)$  as an alternative to the initial-state radiation and energy scan techniques, which relies on positron annihilation off atomic electrons of a high  $Z$  target ( $^{238}\text{U}$ ,  $Z = 92$ ). We show that by leveraging the relativistic electron velocities of the inner atomic shells, a high-intensity 12 GeV positron beam, such as the one foreseen at JLab, can allow to measure  $\sigma_{\text{had}}(s)$  with high statistical accuracy from the two-pion threshold up to above  $\sqrt{s} \sim 1 \text{ GeV}$ .

**Introduction.** Accurate predictions for the muon anomalous magnetic moment  $a_\mu$  [1, 2], when compared with precise experimental measurements, provide a powerful test of the Standard Model (SM). This is because all three SM sectors - QED, Weak, and QCD - contribute to determine its value. Regrettably, while the precise experimental determinations from BNL [3] and FNAL [4, 5] are in excellent agreement, the theoretical situation remains unsatisfactory, as different evaluations yield discordant results.

The hadronic vacuum polarization (HVP), whose contribution to the muon anomalous magnetic moment is commonly denoted as  $a_\mu^{\text{HVP}}$ , involves nonperturbative QCD effects and is, by far, the most complex and least controlled input in the theoretical calculations. Evaluations of the HVP are carried out relying on two different strategies. From first principles, by means of QCD lattice techniques, and via dispersive methods - a data driven approach that uses as input the hadronic cross section  $\sigma_{\text{had}}$  measured in  $e^+e^-$  annihilation. So far, the most precise lattice result has been obtained by the BMW collaboration [6, 7], and no other lattice determinations of the full  $a_\mu^{\text{HVP}}$  with comparable precision are yet available. Nevertheless, the partial contribution  $a_W^{\text{HVP}}$ , that corresponds to the so-called intermediate Euclidean time-distance window, in which lattice-related systematic and statistical uncertainties are under good control, has been evaluated by several other collaborations [8–15]. The results are in good agreement among them and with BMW, giving strong support to the reliability of lattice evaluations.

However, the BMW result is in tension with the recommended value of  $a_\mu^{\text{HVP}}$  derived from  $e^+e^- \rightarrow \text{hadrons}$  cross section data [2] measured at  $e^+e^-$  circular colliders. The tension is exacerbated in the case of  $a_W^{\text{HVP}}$ , for which the dispersive method yields a value [16] that is several

standard deviations below the average of lattice results.<sup>1</sup> The situation is further complicated by the presence of significant disagreements between different experimental determinations of  $\sigma_{\text{had}}$ . The two most precise determinations based on the initial-state radiation (ISR) technique by KLOE [18] and BaBar [19, 20], exhibit a long-standing  $\sim 3\sigma$  discrepancy.<sup>2</sup> This disagreement has been recently overshadowed by the new CMD-3 result [22] obtained by using the energy scan technique, which is well above (and hardly consistent with) the KLOE and BaBar determinations. For example, in the energy range  $\sqrt{s} \in [0.6, 0.88] \text{ GeV}$  the CMD-3 contribution to  $a_\mu^{\text{HVP}}$  is more than  $5\sigma$  above the estimate based on KLOE data. These discrepancies underscore the urgent need for new, accurate determinations of  $\sigma_{\text{had}}$ . The impact of such measurements would be significantly amplified if a novel method, distinct from the ISR and scanning techniques, could be devised to determine the energy dependence of the cross section.<sup>3</sup>

The aim of this work is to propose a new technique to measure  $\sigma_{\text{had}}$  which could be implemented leveraging high energy and high luminosity positron beams that could become readily available in the near future. The strategy is inspired by the recent realization that in positron annihilation on fixed targets, the momentum distribution of atomic electrons allows to scan over a large

<sup>1</sup> The tension between the data driven result [16] and individual results of different lattice collaborations is around  $4\sigma$  [6, 8, 9, 15]. Ref. [9] quotes  $4.5\sigma$  for the combined BMW [6], CLS/Mainz [8], and ETMC [9] estimates neglecting correlations. Ref. [17] quotes a  $3.8\sigma$  tension for the combined BMW, CLS/Mainz, ETMC and RBC/UKQCD [15] assuming 100% correlation.

<sup>2</sup> It has been speculated recently that higher-order QED effects might play a role in this disagreement [21].

<sup>3</sup> The MUon on Electron (MUonE) elastic scattering experiment [23], which aims to determine  $a_\mu^{\text{HVP}}$  using data from elastic muon scattering off atomic electrons in the spacelike region, is a notable example of an alternative strategy.

range of centre-of-mass (c.m.) energies, even when keeping the beam energy fixed [24].<sup>4</sup> In this Letter we consider a target of natural (or depleted) uranium ( $^{238}\text{U}$ ), that has the largest nuclear charge ( $Z = 92$ ) among all natural elements. The relativistic velocities of the electrons in the inner atomic shells allow to effectively probe  $\sigma_{\text{had}}(s)$  at c.m. energies up to  $\sqrt{s} \sim 1 \text{ GeV}$  even with beam energies  $E_b \sim 12 \text{ GeV}$ , that are well below the threshold for  $2\pi$  ( $E_b = 77 \text{ GeV}$ ) and  $2\mu$  ( $E_b = 44 \text{ GeV}$ ) production for positron annihilating off electrons-at-rest.

The letter is organised as follows: we first outline the steps required to account for the atomic electron momentum distribution  $n(k)$  in evaluating the cross section for  $2 \rightarrow 2$  scatterings, concentrating on the process  $e^+e^- \rightarrow \mu^+\mu^-$ . We next describe the methods we have used to evaluate  $n(k)$ , with particular attention to the high momentum tail of the distribution. Finally, we focus on high precision measurements of  $\sigma_{\text{had}}(s)$  achievable via positron annihilation on electrons of a fixed  $^{238}\text{U}$  target. To illustrate our strategy, we explore the potential reach of the 12 GeV positron beam whose development is under study at the Continuous Electron Beam Accelerator Facility (CEBAF) at Jefferson Laboratory (JLab) [26–28], and of a  $O(100) \text{ GeV}$  high-quality positron beam that can be available at the SPS H4 beamline [29, 30] in the CERN North Experimental Area [31]. We argue that in the range  $\sqrt{s} \leq 1 \text{ GeV}$  a statistical precision on  $\sigma_{\text{had}}(s)$  better than the typical benchmarks of circular  $e^+e^-$  colliders can be obtained at the CEBAF facility, while for the CERN H4 beam line an increase of the positron beam luminosity by at least three orders of magnitude would be required to provide a competitive measurement. It is important to stress that the novel technique of exploiting positron annihilation on fixed target for  $\sigma_{\text{had}}(s)$  measurements also has a high degree of complementarity with  $e^+e^-$  colliders measurements, as it provides the largest statistics in the  $\sqrt{s}$  region close to threshold, where collider data are generally affected by large statistical fluctuations.

**Di-muon cross section.** Let us consider the luminosity independent measurement of  $\sigma_{\text{had}}$  that can be obtained from the experimentally measured  $R$ -ratio  $R(s) = N_{\text{had}}(s)/N_{\mu\mu}(s)$  (where  $N_{\text{had}}$  and  $N_{\mu\mu}$  denote respectively the number of hadronic and di-muon events) multiplied by the  $e^+e^- \rightarrow \mu^+\mu^-$  theoretical cross-section:<sup>5</sup>

$$\sigma_{\text{had}}(s) = R(s) \sigma_{\mu\mu}^{\text{th}}(s). \quad (1)$$

<sup>4</sup> The importance of accounting for atomic electron velocities in positron annihilation on fixed target experiments was first highlighted in Ref. [25].

<sup>5</sup> This method has been used for example by the BaBar collaboration [19, 20] and by KLOE in Ref. [32]. It relies on the assumption that  $\sigma_{\mu\mu}^{\text{th}}$  is fully determined by SM processes (see [33, 34] for a counterexample).

The specific process we are interested in is the annihilation of a positron with given energy  $E_B$  and momentum  $\mathbf{p}_B = (0, 0, p_B)$  with an atomic electron in a certain orbital  $n, l$  with momentum-space wavefunction  $\phi_{nl}(\mathbf{k}_A)$ , yielding a di-muon final state  $\mu^-(\mathbf{p}_1) + \mu^+(\mathbf{p}_2)$ . The differential cross section, denoted as  $d\sigma$  for brevity, can be written as:

$$d\sigma = \frac{d^3p_1 d^3p_2 d^3k_A}{(2\pi)^5 16 E_1 E_2} \frac{|\phi_{nl}(\mathbf{k}_A)|^2 |\mathcal{M}|^2}{|E_B k_A^z - E_A p_B|} \times \delta^4(\hat{k}_A + \hat{p}_B - \hat{p}_f), \quad (2)$$

where  $\mathcal{M}$  is the matrix element, and  $\hat{k}_A$ ,  $\hat{p}_B$  and  $\hat{p}_f = \hat{p}_1 + \hat{p}_2$  denote four-momenta. In the energy conservation condition we have neglected the electron binding energy, which is justified given the wide scale separation between binding energies and the c.m. energy in the process.

We can readily integrate over the three-momentum of one muon (e.g.  $\mathbf{p}_1$ ) leaving a single delta function  $\delta(E_A + E_B - (\omega_1 + E_2))$  such that

$$\omega_1 = \sqrt{|\mathbf{p}_1|^2 + m_\mu^2}, \quad p_1^i = k_A^i - p_2^i + p_B \delta_{iz}, \quad (3)$$

with  $i = x, y, z$ . Assuming an isotropic distribution for the electron momentum, we can use spherical coordinates  $d^3k_A = k_A^2 dk_A dc_{\theta_A} d\varphi_A$  and  $d^3p_2 = p_2^2 dp_2 dc_{\theta_2} d\varphi_2$ , where  $c_{\theta_A} = \cos \theta_A$  and  $c_{\theta_2} = \cos \theta_2$ . We can now rewrite

$$\begin{aligned} \omega_1 &= \sqrt{a - b c_{\varphi_2 - \varphi_A}}, \\ a &= p_2^2 + m_\mu^2 + k_A^2 + p_B^2 + 2k_A p_B c_{\theta_A} \\ &\quad - 2p_2 c_{\theta_2} (p_B + k_A c_{\theta_A}), \\ b &= 2k_A p_2 s_{\theta_2} s_{\theta_A}. \end{aligned} \quad (4)$$

Let us define  $\mathcal{E} = E_A + E_B - E_2$ . The integration over  $\varphi_2$  and  $\varphi_A$  can be performed analytically, after rewriting

$$\frac{\delta(\omega_1 - \mathcal{E})}{\omega_1} = 2 \frac{\delta(\varphi_2 - \varphi_2^+) + \delta(\varphi_2 - \varphi_2^-)}{b\sqrt{1 - d^2}}, \quad (5)$$

where  $\varphi_2^\pm = \varphi_A \pm \arccos d$ ,  $d = (a - \mathcal{E}^2)/b$ . This yields

$$\int_0^{2\pi} d\varphi_A \int_0^{2\pi} d\varphi_2 \frac{\delta(\omega_1 - \mathcal{E})}{\omega_1} = \frac{4(2\pi - \arccos d)}{b\sqrt{1 - d^2}} \Pi\left(\frac{d}{2}\right) \quad (6)$$

with  $\Pi(x) = 1$  for  $|x| \leq \frac{1}{2}$  and 0 otherwise. Changing variable from  $c_{\theta_A}$  to  $s = 2m_e^2 + 2(E_B E_A - p_B k_A c_{\theta_A})$ , we finally obtain:

$$\begin{aligned} \frac{d^2\sigma}{ds dc_{\theta_2}} &= \int_{m_\mu}^\infty dE_2 \int_0^\infty dk_A \frac{|\mathcal{M}|^2}{32\pi^2} \frac{|\phi_{nl}(k_A)|^2}{16\pi^3} \\ &\quad \times \frac{(2\pi - \arccos d) \Pi\left(\frac{d}{2}\right)}{p_B |E_B k_A c_{\theta_A} - E_A p_B| s_{\theta_2} s_{\theta_A} \sqrt{1 - d^2}}, \end{aligned} \quad (7)$$

where the  $\Pi$  function, which restricts the integration to values for which  $|d| < 1$  (that in turn implies  $k_A$

larger than a certain  $k_A^{\min}$ ) enforces implicitly energy conservation, and  $c_{\theta_A} = (2m_e^2 + 2E_A E_B - s)/(2p_B k_A)$ ,  $s_{\theta_A} = (1 - c_{\theta_A}^2)^{1/2}$ . The squared matrix element for  $e^+e^- \rightarrow \mu^+\mu^-$  reads

$$\frac{|\mathcal{M}|^2}{32\pi^2} = \alpha^2 \left[ 1 + \frac{2}{s^2} \left( u^2 + u(s - 2(m_e^2 + m_\mu^2)) + (m_e^2 + m_\mu^2)^2 \right) \right], \quad (8)$$

with  $u = m_e^2 + m_\mu^2 - 2(E_B E_2 - p_B p_2 c_{\theta_2})$ .

**Electron momentum distribution.** The differential cross section for dimuon production in positron annihilation off  $^{238}\text{U}$  atomic electrons is obtained by summing Eq. (7) over all electron orbitals, that is by replacing  $|\phi_{n\ell}(k_A)|^2$  with the properly normalised (isotropic) electron momentum distribution:

$$n(k_A) = \sum_{n\ell} |\phi_{n\ell}(k_A)|^2, \quad \int \frac{k_A^2 n(k_A) dk_A}{2\pi^2} = Z, \quad (9)$$

with  $Z = 92$ . For any given material, the electron momentum distributions is related to its isotropic Compton Profile (CP)  $J(k)$  via

$$n(k) = -\frac{(2\pi)^2}{k} \frac{dJ(k)}{dk}. \quad (10)$$

CPs are directly measurable in photon scattering experiments, and provide an important confirmation of *ab initio* theoretical calculations. For our estimates, we adopt the theoretical CP for  $^{238}\text{U}$  given in Ref. [35], where orbital and total-atom CPs are computed for heavy elements using relativistic Dirac-Hartree-Fock wavefunctions, up to  $k = 100$  a.u.  $\simeq 370$  keV. For momenta above 370 keV and up to  $k_A \simeq 11$  MeV we complement the results of [35] by numerically estimating the contribution of the core orbitals up to the  $3d$  shell, using the code DBSR-HF [36]. For even larger momenta we use a simple approximation (valid for  $k_A \gg m_e \alpha Z$ ) which only includes the contribution of the electrons in the  $1s$  shell

$$n^{1s}(k_A) = \frac{32\pi(1 + 1.174 Z^2 \alpha^2)}{Z \alpha m_e^3 x_A^2 (1 + x_A^2)^{1 + \sqrt{1 - Z^2 \alpha^2}}}, \quad (11)$$

where  $x_A = \frac{k_A}{m_e \alpha Z}$  is the reduced momentum and  $Z = 92$  is the (unscreened) nuclear charge for  $1s$  electrons localized close to the nucleus. Finally, we cut-off the momentum distribution at  $k_A \lesssim 26$  MeV, related to the  $^{238}\text{U}$  nuclear radius  $R_U \simeq 7.4$  fm [37], since for electrons localized inside the nucleus our cross-section (especially for hadron production) is no more reliable.<sup>6</sup> This cut also ensures that there is no loss of acceptance related to events

<sup>6</sup> Possible nuclear theoretical uncertainties related to hadron production close to the nucleus can be avoided with a more conservative cut on the momentum distribution, at the cost of reducing the accessible c.m. energy range.

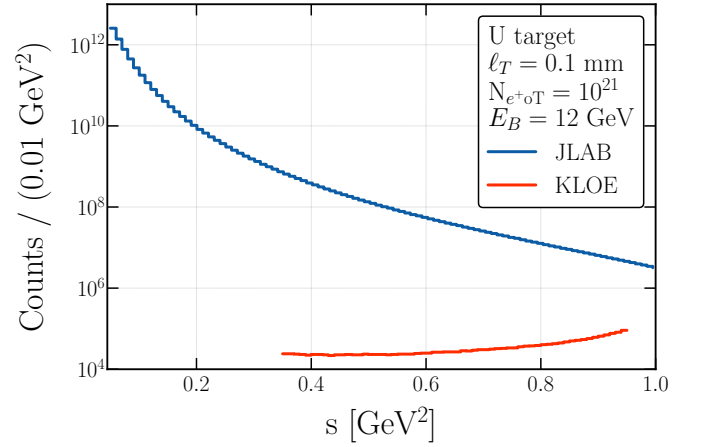


FIG. 1. Number of  $\mu^+\mu^-$  events produced at JLAB with a beam energy of  $E_B = 12$  GeV, compared with the number of  $\mu^+\mu^-\gamma$  events detected by KLOE, as reported in Ref. [32].

with muons propagating backwards, given the threshold  $k_A \gtrsim m_\mu/2$  for such kinematic configurations.

**Statistical procedure.** The HVP contribution to  $a_\mu$  is related to the hadronic cross section via the dispersion integral

$$a_\mu^{\text{HVP}} = \frac{1}{4\pi^3} \int_{4m_\pi^2}^{\infty} ds \sigma_{\text{had}}(s) K(s), \quad (12)$$

with  $K(s) = \int_0^1 dz \frac{z^2(1-z)}{z^2 + s(1-z)/m_\mu^2}$ . The integral is estimated from experimental data by replacing it with a finite sum over bins of width  $\Delta s_i$

$$a_\mu^{\text{HVP}} \simeq \frac{1}{4\pi^3} \sum_i^{n_{\text{bin}}} \Delta s_i \sigma_{\text{had}}(s_i) K(s_i) \equiv \sum_i^{n_{\text{bin}}} a_\mu^i, \quad (13)$$

where  $\sigma_{\pi\pi}(s_i)$  is the cross section at  $s_i$ . Given that  $\sigma_{\text{had}}$  is expressed in terms of the  $R$ -ratio (see Eq. (1)) the statistical uncertainty corresponds to the sum in quadrature of the uncertainties on  $N_{\text{had}}^i$  and  $N_{\mu\mu}^i$  in each bin:

$$\delta a_\mu^{\text{HVP}} = \sqrt{\sum_i^{n_{\text{bin}}} (a_\mu^i)^2 \left[ \left( \frac{\delta N_{\pi\pi}^i}{N_{\pi\pi}^i} \right)^2 + \left( \frac{\delta N_{\mu\mu}^i}{N_{\mu\mu}^i} \right)^2 \right]} \quad (14)$$

where

$$\frac{\delta N_{\mu\mu}(s_i)}{N_{\mu\mu}(s_i)} = \frac{1}{\sqrt{N_{\mu\mu}(s_i)}}, \quad (15)$$

$$\frac{\delta N_{\pi\pi}(s_i)}{N_{\pi\pi}(s_i)} = \frac{1}{\sqrt{R(s_i) N_{\mu\mu}}}$$

**Positron beams and projections.** The CEBAF injector at JLab is anticipated to be capable of producing  $1 - 5 \mu\text{A}$  unpolarized positron beams, and acceleration to

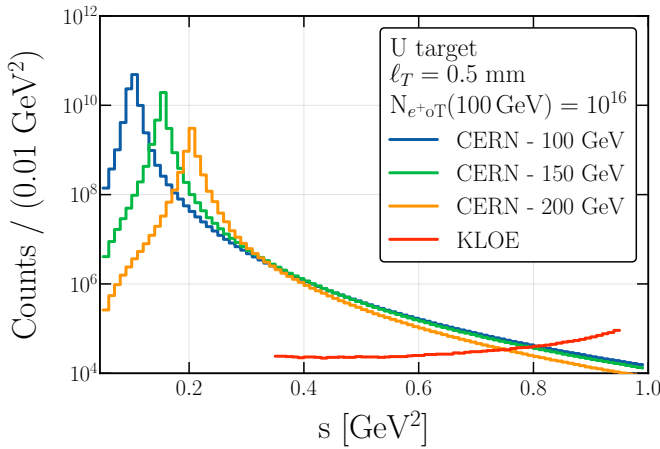


FIG. 2. Number of  $\mu^+\mu^-$  events produced with the CERN H4 line assuming  $N_{e^+oT} \sim 10^{16}$  at  $E_B = 100$  GeV (blue line) and an exponential scaling of the beam intensity as given in Eq. (16) for  $E_B = 150$  GeV (green line) and  $E_B = 200$  GeV (orange line). The red line gives the number of  $\mu^+\mu^-\gamma$  detected by KLOE, as reported in Ref. [32].

energies up to 11–12 GeV. The higher figures quoted are demanding but still realistic [38]. In our study, we have taken  $E_B = 12$  GeV with a negligible energy spread,  $10^{21}$  positrons on target ( $e^+oT$ ) corresponding to one year of data taking with a  $5 \mu A$  positron current, and a thin uranium target of thickness  $\ell_T = 100 \mu m$ . Given that the U radiation length is  $X_0^U \simeq 3.2$  mm, this allows us to neglect  $e^+$  energy losses inside the target. It should be remarked, however, that if the positron current, or the duration of the data taking run, are decreased by a factor of a few, this could be largely compensated by increasing the target thickness by similar factors. Our results are shown in Figure 1. The blue line corresponds to the number of di-muon events, binned in intervals of equal size  $\Delta s_i = 0.01 \text{ GeV}^2$ , that can be produced at JLab. The red line gives for comparison the number of  $\mu^+\mu^-\gamma$  events detected by KLOE, as reported in Ref. [32]. It is apparent that even at c.m. energies of the order of 1 GeV, where the suppression from the electron momentum distribution becomes particularly strong, JLab has still the potentiality of collecting a statistics more than one order of magnitude larger than those of circular  $e^+e^-$  colliders. As a result, the outlined statistical procedure applied to the simulated JLAB dataset in the range  $4m_\pi^2 < s < 1 \text{ GeV}^2$  yields a statistical uncertainty below 0.005%. This clearly implies that the measurement will be dominated by systematic uncertainties.

In the CERN North Experimental Area (NA), positron beams of much higher energy can be available, and it is then natural to ask how a one order of magnitude increase in energy would influence the measurement. The downside, however, is that the NA positron beams are tertiary beams. Spills of 400 GeV protons from the SPS

first impinge on a beryllium target producing all sorts of particles. Charged particles are deflected away, while secondary photons, and photons from  $\pi_0$  decays, pair produce  $e^+e^-$  in a lead converter located downstream. Magnetic fields and collimators are then used for charge and momentum selection. As a result, a typical figure for the CERN H4 line (serving the NA64 experiment) is  $5 \cdot 10^6 e^+oT/spill$  [39]. Assuming 3500 spills/day this would corresponds to  $\sim 6.5 \cdot 10^{12} poT/yr$ , which is not sufficient to allow for a useful measurement. Nevertheless, it remains interesting to explore the energy dependence of the measurement. To this end, we assume an (unrealistic)  $N_{e^+oT} \sim 10^{16}$  for a beam energy  $E_B = 100$  GeV, an energy spread  $\sim 1\%$ , and a  $500 \mu m$  uranium target. To account for the scaling of the beam intensity at energies above 100 GeV we adopt the Gagnon parametrization (see the technical note Ref. [29]), which gives

$$\frac{N_{e^+oT}(p')}{N_{e^+oT}(p)} = e^{-\frac{B}{p_0}(p'-p)}, \quad (16)$$

where  $p_0$  is the energy of the primary protons (400 GeV),  $B = 10$ , and  $N_{e^+oT}(100 \text{ GeV}) = 10^{16}$ . Our results are depicted in Fig. 2 for three values of the positron energy  $E_B = 100, 150, 200$  GeV (respectively blue, green and orange lines). The number of  $\mu^+\mu^-\gamma$  events detected by KLOE, as reported in Ref. [32] is plotted for comparison (red line). In the range  $4m_\pi^2 < s < 0.8 \text{ GeV}^2$  the statistical uncertainty on  $a_\mu^{\text{HVP}}$  associated with our simulated dataset remains below 0.05%. Hence also in this case systematic uncertainties will play the dominant role.

It is intriguing to note that above  $s \sim 0.3 \text{ GeV}^2$ , increasing the beam energy does not result in a gain in statistics. Although for a given value of  $\sqrt{s}$  higher positron energies allows probing smaller electron momenta, where the momentum density distribution is less suppressed, the corresponding decrease in beam intensity, as parametrised in Eq. (16), more than offsets this advantage. Thus, considering that hadron contamination in the positron beams increases from 2–3% at  $E_B = 100$  GeV to more than 100% at  $E_B = 200$  GeV, see Ref. [40], lower beam energies turn out to be preferable. Finally, the result of a measurement with a more realistic  $N_{e^+oT}(100 \text{ GeV}) = 10^{13}$  can easily be inferred by rescaling the blue line in Fig. 2 by a factor  $10^{-3}$ . In this case only the region  $4m_\pi^2 \lesssim s \lesssim 0.3 \text{ GeV}^2$  could be probed with sufficient statistical precision. However, such a measurement would still be of remarkable interest, as it would be complementary to the ISR and energy scan techniques, that in this region exhibit reduced statistics.

**Conclusions.** The novel strategy to measure  $\sigma_{\text{had}}$  that we have proposed could play a pivotal role in solving the conundrum of the discordant determinations of the HVP contribution to the muon anomalous magnetic moment extracted from  $e^+e^- \rightarrow \text{hadrons}$  data. Presently, the most accurate estimates are obtained from measurements



at  $e^+e^-$  circular colliders. Two different techniques are employed to reconstruct the energy dependence of the cross-section: either the scanning method, in which the beam energies are varied, or the radiative return method, in which a hard photon is emitted from the initial state thus modifying the c.m. energy of the collision. We have shown that a different type of measurement can be carried out with positron beams in fixed target experiments. A scan over the c.m. dependence of the cross section is automatically provided by leveraging the atomic electron velocities in high  $Z$  target materials, like  $^{238}\text{U}$ . This method can provide statistically accurate measurements that are complementary to the ones at colliders, as the statistics will be particularly large in the low  $\sqrt{s}$  region around the two pion threshold, where the ISR and scanning method are affected by the largest statistical uncertainties. We have studied the reach of the positron beam foreseen at JLab, and we have shown that with the anticipated beam parameters the whole region from the two-pion threshold up to above  $\sqrt{s} \sim 1 \text{ GeV}$ , that is the crucial one for accurate determinations of  $a_\mu^{\text{HVP}}$ , can be fully covered. Conversely, the positron beams available in the CERN NA do not have a sufficient intensity to cover in full the interesting range. Still, with realistic beam parameters  $\sigma_{\text{had}}(s)$  can be measured with good statistical accuracy in the low energy region  $4m_\pi^2 \lesssim s \lesssim 0.3 \text{ GeV}^2$ . The issue of experimental detection of  $\mu^+\mu^-$  and  $\pi\pi(\gamma)$  events with the related systematic uncertainties is beyond the scope of this work, and it has not been addressed in our study. However, it is clear that to successfully carry out the measurement that we are proposing, it will be required, among other things, a good  $\pi/\mu$  discrimination and an accurate reconstruction of the c.m. energy of the collision from the final states momenta.

**Acknowledgments** – We warmly thank Lau Gatignon and Johannes Bernhard for providing us with detailed information about the CERN NA beams, and Eric Voutier for details on the CEBAF positron beam parameters. We acknowledge conversations with M. Raggi and P. Valente. E.N. acknowledges hospitality from the LAPth group in Annecy during the development of this work. F.A.A., G.G.d.C. and E.N. are supported in part by the INFN “Iniziativa Specifica” Theoretical Astroparticle Physics (TAsP). F.A.A. received additional support from an INFN Cabibbo Fellowship, call 2022. G.G.d.C. acknowledges LNF and Sapienza University for hospitality at various stages of this work. The work of E.N. is also supported by the Estonian Research Council grant PRG1884. Partial support from the CoE grant TK202 “Foundations of the Universe” and from the CERN and ESA Science Consortium of Estonia, grants RVT7 and RVT7, and from the COST (European Cooperation in Science and Technology) Action COSMIC WISPer CA21106 are also acknowledged.

---

\* fernando.ariasaragon@lnf.infn.it

† l.darme@ip2i.in2p3.fr

‡ giovanni.grilli@lngs.infn.it

§ enrico.nardi@lnf.infn.it

- [1] Fred Jegerlehner and Andreas Nyffeler, “The Muon  $g-2$ ,” *Phys. Rept.* **477**, 1–110 (2009), arXiv:0902.3360 [hep-ph].
- [2] T. Aoyama *et al.*, “The anomalous magnetic moment of the muon in the Standard Model,” *Phys. Rept.* **887**, 1–166 (2020), arXiv:2006.04822 [hep-ph].
- [3] G.W. Bennett *et al.* (Muon  $g-2$ ), “Final Report of the Muon E821 Anomalous Magnetic Moment Measurement at BNL,” *Phys. Rev. D* **73**, 072003 (2006), arXiv:hep-ex/0602035.
- [4] B. Abi *et al.* (Muon  $g-2$ ), “Measurement of the Positive Muon Anomalous Magnetic Moment to 0.46 ppm,” *Phys. Rev. Lett.* **126**, 2021 (2021), arXiv:2104.03281 [hep-ex].
- [5] D. P. Aguillard *et al.* (Muon  $g-2$ ), “Measurement of the Positive Muon Anomalous Magnetic Moment to 0.20 ppm,” *Phys. Rev. Lett.* **131**, 161802 (2023), arXiv:2308.06230 [hep-ex].
- [6] Sz. Borsanyi *et al.*, “Leading hadronic contribution to the muon magnetic moment from lattice QCD,” *Nature* **593**, 51–55 (2021), arXiv:2002.12347 [hep-lat].
- [7] A. Boccaletti *et al.*, “High precision calculation of the hadronic vacuum polarisation contribution to the muon anomaly,” (2024), arXiv:2407.10913 [hep-lat].
- [8] Marco Cè *et al.* (ETMC), “Window observable for the hadronic vacuum polarization contribution to the muon  $g-2$  from lattice QCD,” *Phys. Rev. D* **106**, 114502 (2022), arXiv:2206.06582 [hep-lat].
- [9] C. Alexandrou *et al.* (Extended Twisted Mass), “Lattice calculation of the short and intermediate time-distance hadronic vacuum polarization contributions to the muon magnetic moment using twisted-mass fermions,” *Phys. Rev. D* **107**, 074506 (2023), arXiv:2206.15084 [hep-lat].
- [10] Christoph Lehner and Aaron S. Meyer, “Consistency of hadronic vacuum polarization between lattice QCD and the R-ratio,” *Phys. Rev. D* **101**, 074515 (2020), arXiv:2003.04177 [hep-lat].
- [11] Christopher Aubin, Thomas Blum, Maarten Golterman, and Santiago Peris, “Muon anomalous magnetic moment with staggered fermions: Is the lattice spacing small enough?” *Phys. Rev. D* **106**, 054503 (2022), arXiv:2204.12256 [hep-lat].
- [12] Christopher Aubin, Thomas Blum, Cheng Tu, Maarten Golterman, Chulwoo Jung, and Santiago Peris, “Light quark vacuum polarization at the physical point and contribution to the muon  $g-2$ ,” *Phys. Rev. D* **101**, 014503 (2020), arXiv:1905.09307 [hep-lat].
- [13] Gen Wang, Terrence Draper, Keh-Fei Liu, and Yi-Bo Yang (chiQCD), “Muon  $g-2$  with overlap valence fermions,” *Phys. Rev. D* **107**, 034513 (2023), arXiv:2204.01280 [hep-lat].
- [14] Alexei Bazavov *et al.* (Fermilab Lattice, HPQCD, MILC), “Light-quark connected intermediate-window contributions to the muon  $g-2$  hadronic vacuum polarization from lattice QCD,” *Phys. Rev. D* **107**, 114514 (2023), arXiv:2301.08274 [hep-lat].
- [15] T. Blum *et al.* (RBC, UKQCD), “Update of Euclidean windows of the hadronic vacuum polarization,” *Phys. Rev. D* **108**, 054507 (2023), arXiv:2301.08696 [hep-lat].

- [16] G. Colangelo, A. X. El-Khadra, M. Hoferichter, A. Keshavarzi, C. Lehner, P. Stoffer, and T. Teubner, “Data-driven evaluations of Euclidean windows to scrutinize hadronic vacuum polarization,” *Phys. Lett. B* **833**, 137313 (2022), [arXiv:2205.12963 \[hep-ph\]](#).
- [17] Hartmut Wittig, “Progress on  $(g - 2)_\mu$  from lattice QCD.” Talk given at the 57th Rencontres de Moriond, Electroweak Interactions & Unified Theories, La Thuile, Italy (2023).
- [18] A. Anastasi *et al.* (KLOE-2), “Combination of KLOE  $\sigma(e^+e^- \rightarrow \pi^+\pi^-\gamma(\gamma))$  measurements and determination of  $a_\mu^{\pi^+\pi^-}$  in the energy range  $0.10 < s < 0.95$  GeV<sup>2</sup>,” *JHEP* **03**, 173 (2018), [arXiv:1711.03085 \[hep-ex\]](#).
- [19] Bernard Aubert *et al.* (BaBar), “Precise measurement of the  $e^+e^- \rightarrow \pi^+\pi^- (\gamma)$  cross section with the Initial State Radiation method at BABAR,” *Phys. Rev. Lett.* **103**, 231801 (2009), [arXiv:0908.3589 \[hep-ex\]](#).
- [20] J. P. Lees *et al.* (BaBar), “Precise Measurement of the  $e^+e^- \rightarrow \pi^+\pi^-(\gamma)$  Cross Section with the Initial-State Radiation Method at BABAR,” *Phys. Rev. D* **86**, 032013 (2012), [arXiv:1205.2228 \[hep-ex\]](#).
- [21] J. P. Lees *et al.* (BaBar), “Measurement of additional radiation in the initial-state-radiation processes  $e^+e^- \rightarrow \mu^+\mu^-\gamma$  and  $e^+e^- \rightarrow \pi^+\pi^-\gamma$  at BABAR,” *Phys. Rev. D* **108**, L111103 (2023), [arXiv:2308.05233 \[hep-ex\]](#).
- [22] F. V. Ignatov *et al.* (CMD-3), “Measurement of the  $e^+e^- \rightarrow \pi^+\pi^-$  cross section from threshold to 1.2 GeV with the CMD-3 detector,” *Phys. Rev. D* **109**, 112002 (2024), [arXiv:2302.08834 \[hep-ex\]](#).
- [23] G. Abbiendi *et al.*, “Measuring the leading hadronic contribution to the muon  $g-2$  via  $\mu e$  scattering,” *Eur. Phys. J. C* **77**, 139 (2017), [arXiv:1609.08987 \[hep-ex\]](#).
- [24] Fernando Arias-Aragón, Luc Darmé, Giovanni Grilli di Cortona, and Enrico Nardi, “Production of Dark Sector Particles via Resonant Positron Annihilation on Atomic Electrons,” *Phys. Rev. Lett.* **132**, 261801 (2024), [arXiv:2403.15387 \[hep-ph\]](#).
- [25] Enrico Nardi, Cristian D. R. Carvajal, Anish Ghoshal, Davide Meloni, and Mauro Raggi, “Resonant production of dark photons in positron beam dump experiments,” *Phys. Rev. D* **97**, 095004 (2018), [arXiv:1802.04756 \[hep-ph\]](#).
- [26] Andrei Afanasev *et al.*, “Physics with Positron Beams at Jefferson Lab 12 GeV,” (2019), [arXiv:1906.09419 \[nucl-ex\]](#).
- [27] A. Accardi *et al.*, “An experimental program with high duty-cycle polarized and unpolarized positron beams at Jefferson Lab,” *Eur. Phys. J. A* **57**, 261 (2021), [arXiv:2007.15081 \[nucl-ex\]](#).
- [28] J. Arrington *et al.*, “Physics with CEBAF at 12 GeV and future opportunities,” *Prog. Part. Nucl. Phys.* **127**, 103985 (2022), [arXiv:2112.00060 \[nucl-ex\]](#).
- [29] Lau Gatignon, “Design and Tuning of Secondary Beamlines in the CERN North and East Areas,” (2020), [10.17181/CERN.T6FT.6UDG](#).
- [30] Sergei; et al. Gninenko, *Light dark matter search with positron beams at NA64*, Tech. Rep. (CERN, Geneva, 2024).
- [31] Dipanwita Banerjee, Johannes Bernhard, Markus Brugger, Nikolaos Charitonidis, Niels Doble, Lau Gatignon, and Alexander Gerbershagen, “The North Experimental Area at the Cern Super Proton Synchrotron,” (2021), [10.17181/CERN.GP3K.0S1Y](#), dedicated to Giorgio Brianti on the 50th anniversary of his founding the SPS Experimental Areas Group of CERN-Lab II and hence initiating the present Enterprise.
- [32] D. Babusi *et al.* (KLOE), “Precision measurement of  $\sigma(e^+e^- \rightarrow \pi^+\pi^-\gamma)/\sigma(e^+e^- \rightarrow \mu^+\mu^-\gamma)$  and determination of the  $\pi^+\pi^-$  contribution to the muon anomaly with the KLOE detector,” *Phys. Lett. B* **720**, 336–343 (2013), [arXiv:1212.4524 \[hep-ex\]](#).
- [33] Luc Darmé, Giovanni Grilli di Cortona, and Enrico Nardi, “The muon  $g - 2$  anomaly confronts new physics in  $e$  and  $\mu$  final states scattering,” *JHEP* **06**, 122 (2022), [arXiv:2112.09139 \[hep-ph\]](#).
- [34] Luc Darmé, Giovanni Grilli di Cortona, and Enrico Nardi, “Indirect new physics effects on  $\sigma_{\text{had}}$  confront the  $(g-2)_\mu$  window discrepancies and the CMD-3 result,” *Phys. Rev. D* **108**, 095056 (2023), [arXiv:2212.03877 \[hep-ph\]](#).
- [35] F. Biggs, L.B. Mendelsohn, and J.B. Mann, “Hartree-fock compton profiles for the elements,” *Atomic Data and Nuclear Data Tables* **16**, 201–309 (1975).
- [36] Oleg Zatsarinny and Charlotte Froese Fischer, “Dbsr\_hf: A b-spline dirac-hartree-fock program,” *Computer Physics Communications* **202**, 287–303 (2016).
- [37] John Markus Blatt and Victor Frederick Weisskopf, *Theoretical nuclear physics* (Springer, New York, 1952).
- [38] Eric Voutier, private communication.
- [39] Johannes Bernhard and Lau Gatignon, private communication.
- [40] Yu. M. Andreev *et al.*, “Measurement of the intrinsic hadronic contamination in the NA64–e high-purity  $e^+/e^-$  beam at CERN,” *Nucl. Instrum. Meth. A* **1057**, 168776 (2023), [arXiv:2305.19411 \[hep-ex\]](#).